AGU PUBLICATIONS

Geophysical Research Letters

RESEARCH LETTER
10.1002/2016GL068302

Key Points:
- Fast and reliable calculation of the moment tensor
- Use of seismogeodesy as a powerful tool for tsunami early warning
- Reducing time for tsunami early warning purposes

Supporting Information:
- Supporting Information S1

Correspondence to:
S. Riquelme,
sebastian@dgf.uchile.cl

Citation:
Riquelme, S., F. Bravo, D. Melgar, R. Benavente, J. Geng, S. Barrientos, and J. Campos (2016), *W* phase source inversion using high-rate regional GPS data for large earthquakes, *Geophys. Res. Lett.*, *43*, 3178–3185, doi:10.1002/2016GL068302.

Received 19 FEB 2016
Accepted 11 MAR 2016
Accepted article online 18 MAR 2016
Published online 6 APR 2016

W phase source inversion using high-rate regional GPS data for large earthquakes

S. Riquelme[1], F. Bravo[2], D. Melgar[3], R. Benavente[4], J. Geng[5], S. Barrientos[1], and J. Campos[2]

[1]National Seismological Center, University of Chile, Santiago, Chile, [2]Geophysics Department, University of Chile, Santiago, Chile, [3]Seismological Laboratory, University of California, Berkeley, California, USA, [4]Research School of Earth Sciences, Australian National University, Canberra, ACT, Australia, [5]GNSS Center, Wuhan University, Wuhan, China

Abstract *W* phase moment tensor inversion has proven to be a reliable method for rapid characterization of large earthquakes. For global purposes it is used at the United States Geological Survey, Pacific Tsunami Warning Center, and Institut de Physique du Globe de Strasbourg. These implementations provide moment tensors within 30–60 min after the origin time of moderate and large worldwide earthquakes. Currently, the method relies on broadband seismometers, which clip in the near field. To ameliorate this, we extend the algorithm to regional records from high-rate GPS data and retrospectively apply it to six large earthquakes that occurred in the past 5 years in areas with relatively dense station coverage. These events show that the solutions could potentially be available 4–5 min from origin time. Continuously improving GPS station availability and real-time positioning solutions will provide significant enhancements to the algorithm.

1. Introduction

The *W* phase was discovered after the 1992 M_w 7.7 Nicaragua earthquake [*Kanamori*, 1993]. It is a long-period wave arriving between *P* and *S* waves that can be synthesized by normal modes (fundamental mode and first overtones of spheroidal modes). In ray theory, it represents a combination of *P*, *PP*, *S*, and *SS* phases. *Kanamori and Rivera* [2008] demonstrated that for large events, it is possible to calculate the full moment tensor for large earthquakes using the *W* phase. *Hayes et al.* [2009] extended the algorithm to lower magnitudes and *Duputel et al.* [2012], calculated the centroid moment tensor (CMT) based on the *W* phase method for a complete catalog of events with magnitude 6.5 and above. That work also proposed new band-pass filters for lower magnitude events. *Benavente and Cummins* [2013] recently used the *W* phase to obtain the Finite Fault Model for the Maule and Tohoku earthquakes. Other recent improvements are discussed in *Nealy and Hayes* [2015]; they have performed the full moment tensor inversion for complex earthquakes, discriminating if the earthquake is single or a double point source using Akaike's Information Criteria.

From an operational point of view, *W* phase has proven to be reliable and robust, being implemented in real time at National Earthquake Information Center, Pacific Tsunami Warning Center, and Institute De Pysique Du Globle de Strabourg. In Chile, it has been implemented at the Centro Sismologico Nacional (CSN) using broadband stations at regional distances in real time since 2011. At CSN the processing flow is as follows: the first *W* phase solution is obtained 5–6 min after the earthquake origin time (OT), it is then recalculated after another 5 min (OT + 10 min), and then again every 5 min four more times (OT + 15, 20, 25, and 30 min). The threshold magnitude was initially M_w 6.5 in 2011 and is M_w 5.0 today (www.csn.uchile.cl/wphase/).

For subduction zones close to coastlines, like many areas in the circum-Pacific region, it is very important to issue a fast local tsunami warning. In particular, as an example, Chile is located in one of the most active seismic regions in the world. On average, every 5 years this region produces a magnitude 7 or above earthquake and every 10 years a magnitude 8 or above event [*Madariaga*, 1998]. With Chile being such a tectonically active country and prone to produce large tsunamis, it is imperative to characterize earthquakes as fast as possible, for instance, the 1960 M_w 9.5 Valdivia earthquake and the 2010 M_w 8.8. Maule earthquake had near-field runups larger than 20 m [*Fritz et al.*, 2011; *Lockridge and Smith*, 1984].

Early warning can include the use of regional accelerometer (strong motion) data, but there are a few limitations with this data type; they cannot capture the low-frequency portion of ground motion in real time, and thus, the double integration is not accurate enough to obtain displacements unambiguously.

It is necessary to have a collocated GPS to constrain the long-period displacement and constrain the integration to match the static offset. Collectively, these problems are referred to as baseline offsets and are mostly due to tilting of the inertial sensor. This inability to record long-period motions leads to magnitude saturation in the near field. On the other hand, broadband seismometers saturate in the near field, rendering them not useful for determining earthquake parameters such as mechanism and magnitude. GPS instruments, while noisier than the aforementioned seismic sensors, overcome all these limitations for large earthquake characterization.

Better understanding of GPS and broadband real-time seismology has led to the development of new methods for tsunami early warning based on these geodetic data [*Crowell et al*., 2012; *Ohta et al*., 2012; *Melgar et al*., 2015, 2016]. It is important to note that in tsunami early warning contexts there is more time to issue an alert than in earthquake early warning systems designed to alert in advance of strong shaking. Thus, it is possible to use more rigorous methods to calculate seismic moment and mechanism for large earthquakes.

Observations from broadband seismometers for the 1992 M_w 7.7 Nicaragua earthquake and the 1994 M_w 8.3 Bolivia earthquake have shown that it is possible to measure long-period near-field energy radiated from these earthquakes. Particularly for the 1994 event, data from the Broadband Andean Joint experiment array, located just above the earthquake, led many authors to note a static offset that was interpreted as near-field displacement. *Ekström* [1995] calculated this near-field displacement, using normal mode theory matching the displacement between *P* and *S* waves (*W* phase). *Vidale et al*. [1995] identified this as long-period energy radiating from the earthquake and pointed out that displacements produced by the source are not strongly affected by Earth structure due to its long wavelength. *Jiao et al*. [1995] interpreted the static offset in the same way. The observations presented in these studies confirm that the *W* phase can be observed at regional distances (up to 10°) and intermediate and far-field distances [*Cummins*, 1997]. This implies that from long-period measurements at these short distances it should be feasible to invert for focal mechanisms and to use this information to drive estimates of the tsunamigenic potential of any earthquake [i.e., *Melgar et al*., 2016].

GPS instruments have the capability to detect this long-period wave directly from displacement measurements in the near field (up to 10°) for large earthquakes. An example for station Catapilco (CATA) during the 2015 M_w 8.3 Illapel, Chile, earthquake is shown in Figure 1. This advantage of GPS instruments allows us to retrieve the *W* phase and then perform a moment tensor inversion. Following, we show the results of the *W* phase centroid moment tensor (WCMT) calculations using GPS at near-field distances for six large events. *Rivera et al*. [2011] calculated the *W* phase centroid moment tensor using regional GPS data for the M_w 9.0 Tohoku-oki, Japan, earthquake. Here we extended this work to the 2010 M_w 7.2 El Mayor-Cucapah, Mexico, earthquake; the 2010 M_w 8.8 Maule, Chile, earthquake; the 2014 M_w 8.2 Iquique, Chile, earthquake and its large M_w 7.8 aftershock; and the 2015 M_w 8.3 Illapel, Chile, earthquake.

2. Data and Methods

We used three components of high-rate GPS data, sampled at 1 s for the earthquakes mentioned in section 1. For all events we use Precise Point positioning with Ambiguity Resolution displacements [*Geng et al*., 2013].

For countries located in subduction zones it is very important to estimate the tsunamigenic potential from large earthquakes as soon as possible. The distance between coast and earthquake source and the slow propagation time of tsunami waves compared to elastic waves, allows for the possibility to reduce the calculation time for magnitude and mechanism with GPS instruments where the *W* phase can be observed in the near field. In this method we employ a *W* phase preliminary magnitude (Output Level 1 in *Duputel et al*. [2012]) to start the moment tensor inversion (Output Level 2 in *Duputel et al*. [2012]). Originally, in *Duputel et al*. [2012] this preliminary magnitude is obtained from broadband stations located between 5° and 50°. Here we use the *W* phase amplitude at the GPS station to compute the preliminary magnitude and then trigger the following steps of the inversion. It is worth mentioning that a preliminary moment magnitude can also be calculated without saturation in the first 1–2 min using the scaling of peak ground displacement (PGD) at regional GPS stations [*Melgar et al*., 2015]. This PGD magnitude can also trigger the moment tensor inversion. In the next section, we compare our results with this methodology.

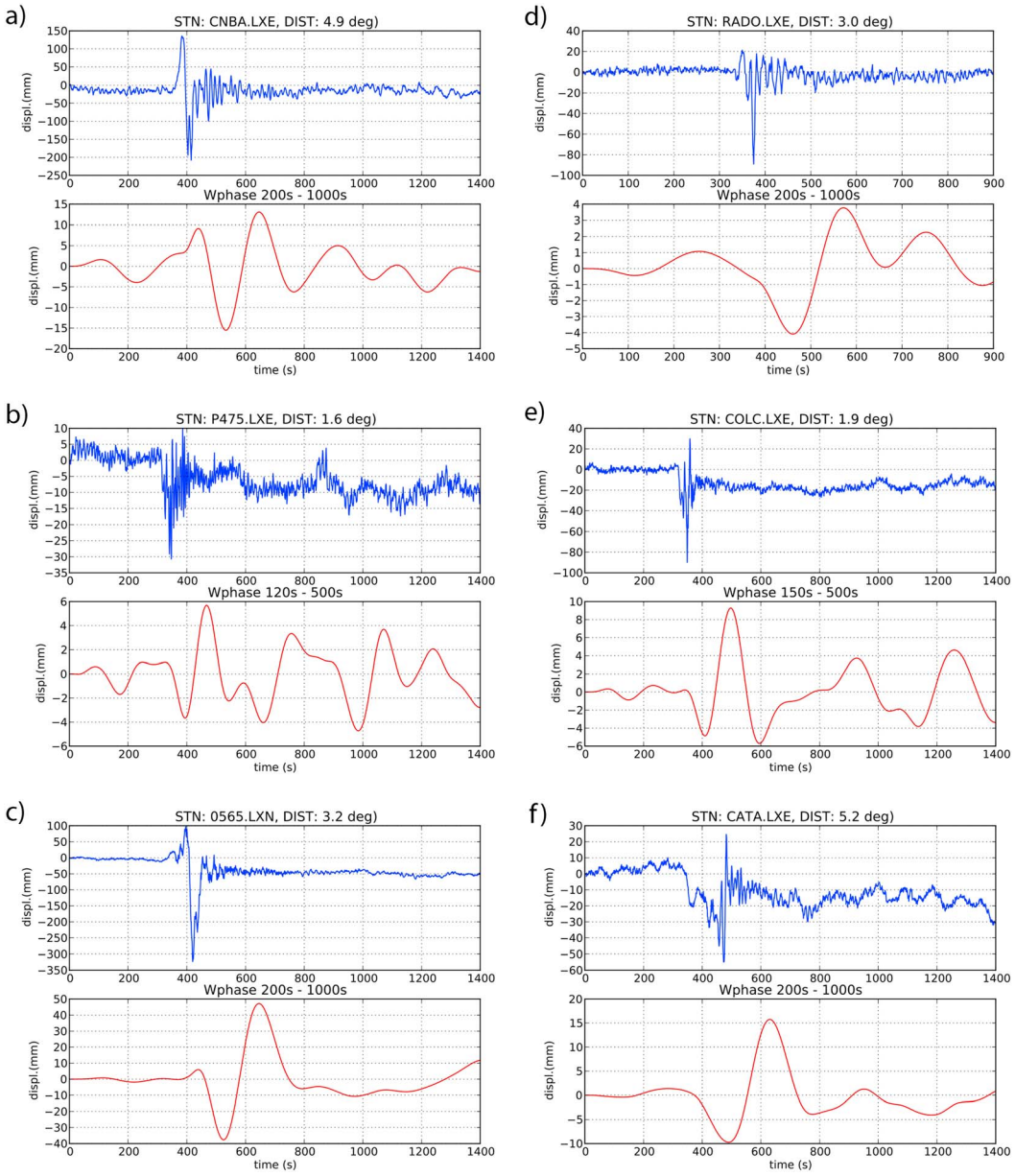

Figure 1. Displacement measured at different stations during each earthquake (blue). *W* phase retrieved from these stations after band-pass filtering using the filters defined in Table 1 (red). Events: (a) Maule earthquake, (b) El Mayor-Cucapah earthquake, (c) Tohoku-oki earthquake, (d) Iquique earthquake, (e) Iquique aftershock, and (f) Illapel earthquake. DIST, distance from the hypocenter in degrees.

Since GPS records do not clip in the near field and faithfully record long periods, for large earthquakes, the early observations of the *W* phase made in the near field (see section 1) allow us to retrieve the focal mechanism as close as the instruments are located to the epicenter. We note that it is important not to incorporate data too close where the point source approximation is not appropriate and finite fault effects can be observed and affect the solution. For example, if a displacement recording is too close to a large slip patch the magnitude will be overestimated. For earthquakes above magnitude 8 in this study we chose a distance range from 2°.

The teleseismic *W* phase inversion uses a time window from T_p to $T_p + 15\Delta$, where T_p is the *p* wave arrival time in seconds and Δ is the distance from the epicenter to a given station in degrees. This time window was originally designed to avoid large amplitude surface waves, which may clip the records even at teleseismic distances [*Duputel et al.* [2012]; *Kanamori and Rivera* [2008]]. The use of GPS data naturally prevents the

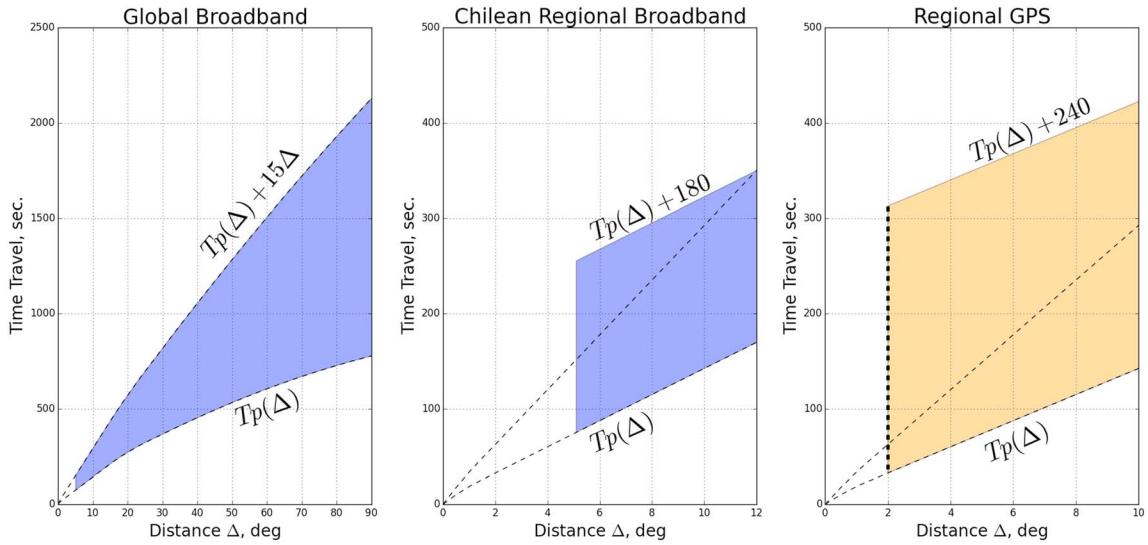

Figure 2. Time window comparison between (a) teleseismic inversion with seismometers, (b) regional inversion with seismometers, and (c) this study, regional inversion with GPS. Figure 2a uses $[T_p, T_p + 15 \times \Delta]$, where Δ is the station to centroid distance in degrees from 5°to 90°, Figure 2b uses a constant window of 180 s with Δ between 5° to 12° distance, and Figure 2c uses a constant window of 240 s for Δ between 2° and 10°; the blue line shows distance when broadband seismometers can be incorporated.

clipping of the records allowing for a longer time window. This is crucial for our regional implementation since utilizing the original *W* phase time window will result in an extremely limited number of observations that can be used in the inversion. In this work we use a constant time window for each station, irrespective of its epicentral distance. A comparison of *W* phase time windows used in different studies can be found in Figure 2.

In the near field, the *P* and *S* waves are very close to each other, making it necessary to test time windows of different lengths to ensure that there is enough *W* phase data to perform the inversion. Another important reason for testing different time windows is the source duration. The 2011 M_w 9.1 Tohoku earthquake had a source time function of ~200 s [*Hayes et al*., 2011]. Thus, this event was still radiating energy while the instruments were recording displacement. This can lead to an increase in the estimated magnitude as time elapses. Therefore, it is necessary to wait for a longer window of *W* phase. Here we tested the method with 1, 2, 3, and 4 min long windows after each earthquake in order to reduce the time for tsunami early warning purposes. In most cases, the inversion is stable at 4 min. This is the original time window proposed by *Rivera et al*., 2011 for the Tohoku earthquake. We used the same filters proposed by *Duputel et al*. [2012] (Table 1), these ones are applied in real time based on a calculated preliminary magnitude. Since the inversion is performed in the time domain, those filters can be used as soon as *W* phase is developed in seismic broadband records. The full inversion is computed in 10 to 30 s, depending on the number of stations. We fix the location of the centroid to the preliminary hypocenter location obtained by the United States Geological Survey (USGS) and assume a half duration from the preliminary magnitude as described in *Kanamori and Rivera* [2008]. We then perform a grid search for the best time shift. Finally, we optimize for the centroid position using a half duration equal to the optimal time shift (Output Level 3 in *Duputel et al*. [2012]). We tested including stations from several distance ranges as well. The inversion is stable with stations no closer than 2° (for earthquakes above magnitude 8), thus ensuring there are no significant finite fault effects in displacements records.

Since GPS stations measure displacement directly, the comparison between observed data and Green's functions is direct; there is no need for instrument response correction. In the original method it is necessary to derive velocity to acceleration and then integrate twice to obtain displacement. For GPS records we only need their a priori position (latitude, longitude, and height) to rotate the time series from geodetic coordinates (Earth-centered, Earth-fixed, or *XYZ*) to local north, east, and up.

Table 1. Filters Used in This Inversion

Magnitude Range	Band-Pass Filter (s)
$M_w >= 8.0$	200–1000
$8.0 > M_w >= 7.5$	150–500
$7.5 > M_w >= 7.0$	120–500

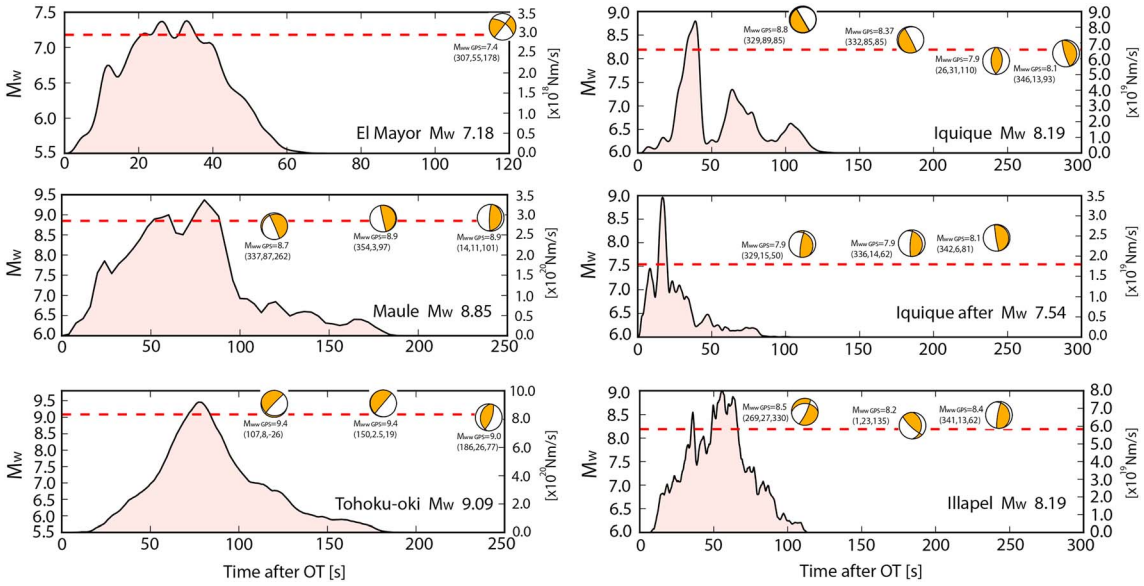

Figure 3. Source time function for each earthquake *modified from Melgar et al.* [2015]. The red dashed line corresponds to the calculated magnitude with PGD. Mechanisms calculated with a time window of 120, 180, and 240 s. For the Maule, Tohoku, and Illapel events the inversion is stable at 240 s. For the events with lower magnitude, it seems possible to use a shorter time window. The Iquique event needed a time window of 290 s to be accurate; however, it is possible to recognize a thrust mechanism at 240 s. *W* phase GPS magnitude over mechanism in parenthesis.

3. Results

Here we present the moment tensor inversion results for each earthquake. We compared moment, moment magnitude, and mechanism with the postprocessed results obtained by the USGS. To validate the mechanisms obtained, we used the methodology proposed by *Kagan* [1991]. We consider an estimation of the moment tensor to be accurate when the rotation angle is less than 35° and the difference in magnitude is less than 0.2.

The 2010 M_w 7.2 El Mayor-Cucapah earthquake shows a transform mechanism that compares well with the USGS *W* phase inversion. The seismic moment calculated for this event is 1.50E+27 dyn cm and $M_w = 7.4$. It shows a plane with strike = 307, dip = 55, and rake = 34.7. The centroid is calculated at latitude = 32.30°N, longitude = 115.40°W, and depth = 12 km. The time shift and centroid delay for this event are 7 s. For the inversion we used a time window of 120 s. The inversion was performed with 20 stations and channels.

The Maule earthquake shows a mechanism with a plane strike = 32.7, dip = 6.9, and rake = 119.6; the seismic moment for this event is 3.21E+29 dyn cm and $M_w = 8.9$; the time window used is 240 s. The inversion was performed with 11 stations and 16 channels. The centroid delay and half duration are 53 s. The centroid is calculated at latitude = 36.12°S, longitude = 72.90°W, and depth = 25.5 km.

For the Tohoku-oki earthquake we obtain a fault plane defined by strike = 20.7, dip = 65.0, and rake = 96.2 and magnitude of $M_w = 9.0$ and a seismic moment of 3.95E+29 dyn cm. This event is by far the most instrumented with the most records available for the inversion with 375 stations and 534 channels. The centroid delay and half duration are 80 s. The centroid is calculated at latitude = 38.29°N, longitude = 142.37°E, and depth = 29.5 km. The time window for the inversion was 240 s.

For the Iquique earthquake the fault plane is the defined by strike = 346, dip = 13, and rake = 93, with a $M_w = 8.1$ and a seismic moment of 1.5 E+28 dyn cm; the centroid coordinates are latitude = 19.70°S, longitude = 70.81°W, and depth = 25.5 km; at 240 s (Figure 3) we observe a thrust mechanism but the best fit of the moment tensor is obtained at 290 s. The centroid delay and half duration are 20 s.

For the Iquique Aftershock we obtained a plane with strike = 336.2, dip = 14.7, and rake = 62.3 with a moment magnitude of $M_w = 7.9$ and a seismic moment of 1.0E+28 dyn cm. The time window of the inversion is 180 s; also, it works accurately for 240 s (Figure 3). The centroid delay and half duration are 10 s. The centroid is located at latitude = 20.40°S, longitude = 70.24°W, and depth = 35.5 km.

Table 2. Summary of Results for Each Earthquake[a]

Earthquake	Mww USGS	MwPGD	Mww GPS	Focal Mechanism USGS	Focal Mechanism WGPS	Number of Stations and Channels	Gap °	Angular Parameter & Mww
El Mayor, Mexico	7.2	7.18	**7.4**	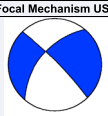 NP1 = (222.0,52.9,-9.7) NP2 =(319.5,82.3,-142.5)	 NP1 = (37.9,88.4,34.7) NP2 =(306.8,55.3,178.1)	28 & 31	211	33.87° & 0.2
Maule, Chile	8.8	8.85	**8.9**	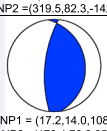 NP1 = (17.2,14.0,108.4) NP2 =(178.4,76.8,85.5)	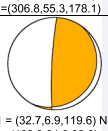 NP1 = (32.7,6.9,119.6) NP2 =(182.9,84.0,86.6)	12 & 20	343	8.43° & 0.1
Tohoku, Japan	9	9.09	**9.0**	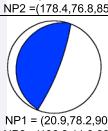 NP1 = (20.9,78.2,90.9) NP2 =(196.3,11.9,88.5)	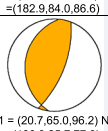 NP1 = (20.7,65.0,96.2) NP2 =(186.3,25.7,77.0)	375 & 534	171	17.04° & 0.0
Iquique, Chile	8.2	8.19	**8.1**	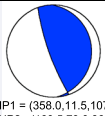 NP1 = (358.0,11.5,107.1) NP2 =(160.5,79.0,86.6)	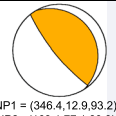 NP1 = (346.4,12.9,93.2) NP2 =(163.1,77.1,89.3)	9 & 9	213	13.56° & 0.1
Iquique Aftershock , Chile	7.7	7.5	**7.9**	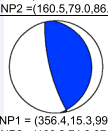 NP1 = (356.4,15.3,99.9) NP2 =(166.2,74.9,87.3)	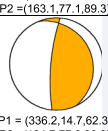 NP1 = (336.2,14.7,62.3) NP2 =(184.7,77.0,96.9)	14 & 29	188	20.23° & 0.2
Illapel, Chile	8.3	8.19	**8.4**	 NP1 = (351.9,22.5,77.3) NP2 =(185.6,68.1,95.2)	 NP1 = (341.2,13.3,62.0) NP2 =(189.9,78.3,96.3)	15 &18	118	23.27° & 0.1

[a]Mww: moment magnitude obtained from *W* phase. Mww obtained from USGS, MwPGD [*Melgar et al*., 2015], and Mww GPS moment magnitude obtained with GPS. Focal mechanisms in blue obtained by USGS COMCAT. Focal mechanisms in orange from this study. Number of stations and channels used for each earthquake. Gap is the azimuthal gap in the inversion. Angular parameter defined by *Kagan* [1991] and delta M_w the difference between Mww and Mww GPS.

For the Illapel earthquake we obtained a thrust mechanism with strike = 341.2, dip = 13.3, and rake = 62.0 and a seismic moment of 5.71E+28 dyn cm. The centroid delay and half duration are 45 s. The calculated moment magnitude is $M_w = 8.36$. The centroid is located at latitude = 31.28°S, longitude = 71.77°W, and depth = 23.5 km. The time window for the inversion was 240 s.

Table 2 summarizes our results and the comparison to the USGS *W* phase inversions. All the moment magnitudes are within ±0.2 magnitude units from the postprocessed calculation and the Kagan rotation angles are less than 35° for all events.

4. Discussion

Time window length seems to be critical for the inversion results in some cases (Figure 3 and waveforms fit in the supporting information). For example, for the El Mayor event the inversion is stable after 120 s, for the Maule, Tohoku, Iquique Aftershock and Illapel earthquakes the inversion is accurate by 240 s, however, the Iquique earthquake needs a time window of 290 s to perform a better estimation of mechanism. For lower magnitudes, like the M_w 7.2 El Mayor-Cucapah or the large M_w 7.8 aftershock from the Iquique event, it is possible to use shorter time windows. Continued study of future earthquakes will show whether this is a general conclusion. It is important to note that the number of stations used in this work is comparatively small; we used less than 20 for the events in Chile, while for the El Mayor-Cucapah we used 28; the exception is Tohoku-oki event where we used 375. This is notable because in teleseismic *W* phase inversion, where worldwide networks of broadband stations are available, inversion is always performed with many more than 20–30 stations. It is remarkable that the method still performs accurately with a smaller number of stations; this suggests that it could be successfully implemented by countries with modest GPS networks. Another factor here is the azimuthal coverage of stations, the teleseismic inversion in most of the cases include a set of stations with a small azimuthal gap, here instead we are using a GPS station distribution

that is one sided, either to the east or west for the Japanese and Chilean cases, respectively. Even for the El Mayor-Cucapah earthquake which is on land all the stations are north from the location of the event. Despite this unfavorable observation geometry, we still obtain reliable mechanisms and magnitudes. Variations compared to WCMT from USGS are likely due to local structure mismodeling, limited number of stations used, and azimuthal coverage.

In light of these considerations we suggest that methodologies that use GPS have an important role to play in tsunami early warning. For all events studied here the results are available within 5 min of event origin time (4 min + delay). This is well within the time frame where the information can be used in advance of the first arrivals of destructive tsunami waves to the local shores. Rapid magnitude determination from the scaling of peak ground displacement (PGD) at GPS stations for these events produces results within ~120 s of event origin time [*Melgar et al*., 2015], somewhat sooner than the *W* phase inversion discussed here. However, calculation of the focal mechanism is not far behind this rapid magnitude calculation and has significant value. It allows monitoring agencies to better manage warnings as they can discern between different kinds of tsunamigenic events (megathrust or outer rise normal faults) and nontsunamigenic events such as strike slip faulting earthquakes which are also possible in close proximity to subduction zones. Thus, this algorithm allows for a cascading approach to warning [*Melgar et al*., 2016]. A rapid magnitude would be available first and could be used to guide initial warnings and decision making by emergency managers while the full focal mechanism that provides a clearer picture of the unfolding hazard would be available only a few minutes afterward and would serve to further refine the warnings and actions of monitoring agencies.

5. Conclusions

Using this algorithm and signals from high-rate, GPS it is possible to calculate the full moment tensor in the near field, potentially 4 min after each large earthquake. However, the earthquake has to be large enough to develop a *W* phase above the current noise threshold (~2 cm) of GPS instruments. We calculated the full moment tensor for six earthquakes above M_w 7.2. It is necessary to test more earthquakes to study if this algorithm can be extended to earthquakes with lower magnitudes. Our results show that this can be done in regions with GPS networks in the near field from 2° to 10° using a time window of 240 s, therefore, from the algorithm point of view, it is an advantage to have the source close to the GPS networks. With more GPS data available and the possibility of including real-time processing, solutions will have significant improvements.

Acknowledgments
We thank the Scripps Orbit and Permanent Array Center (SOPAC) for access to the El Mayor-Cucapah GPS data and the Geospatial Information Authority (GSI) for the Tohoku-oki data. We thank Luis Rivera for his support and insights at the beginning of this work. We thank Paul Bodin and an anonymous reviewer for their helpful comments.

References

Benavente, R., and P. R. Cummins (2013), Simple and reliable finite fault solutions for large earthquakes using the W-phase: The Maule (M_w = 8.8) and Tohoku (M_w = 9.0) earthquakes, *Geophys. Res. Lett.*, *40*, 3591–3595, doi:10.1002/grl.50648.

Crowell, B. W., Y. Bock, and D. Melgar (2012), Real-time inversion of GPS data for finite fault modeling and rapid hazard assessment, *Geophys. Res. Lett.*, *39*, L09305, doi:10.1029/2012GL051318.

Cummins, P. R. (1997), Earthquake near field and W phase observations at teleseismic distances, *Geophys. Res. Lett.*, *24*(22), 2857–2860, doi:10.1029/97GL52960.

Duputel, Z., L. Rivera, H. Kanamori, and G. Hayes (2012), W phase source inversion for moderate to large earthquakes (1990–2010), *Geophys. J. Int.*, *189*, 1125–1147.

Ekström, G. (1995), Calculation of static deformation following the Bolivia earthquake by summation of Earth's normal modes, *Geophys. Res. Lett.*, *22*(16), 2289–2292, doi:10.1029/95GL01435.

Fritz, H., et al. (2011), Field survey of the 27 February 2010 Chile tsunami, *Pure Appl. Geophys.*, *168*(11), 1989–2010.

Geng, J., Y. Bock, D. Melgar, B. W. Crowell, and J. S. Haase (2013), A new seismogeodetic approach applied to GPS and accelerometer observations of the 2012 Brawley seismic swarm: Implications for earthquake early warning, *Geochem. Geophys. Geosyst.*, *14*, 2124–2142, doi:10.1002/ggge.20144.

Hayes, G. P., L. Rivera, and H. Kanamori (2009), Source inversion of the W-Phase: Real-time implementation and extension to low magnitudes, *Seismol. Res. Lett.*, *80*(5), 817–822.

Hayes, G. P., P. S. Earle, H. M. Benz, D. J. Wald, and R. W. Briggs (2011), 88 hours: The US Geological Survey National Earthquake Information Center Response to the 11 March 2011 M_w 9.0 Tohoku earthquake, *Seismol. Res. Lett.*, *82*(4), 481–493.

Jiao, W., T. C. Wallace, S. L. Beck, P. G. Silver, and G. Zandt (1995), Evidence for static displacements from the June 9, 1994 deep Bolivian earthquake, *Geophys. Res. Lett.*, *22*(16), 2285–2288, doi:10.1029/95GL02071.

Kagan, Y. Y. (1991), 3-D rotation of double-couple earthquake sources, *Geophys. J. Int.*, *106*(3), 709–716.

Kanamori, H. (1993), W phase, *Geophys. Res. Lett.*, *20*, 1691–1694, doi:10.1029/93GL01883.

Kanamori, H., and L. Rivera (2008), Source inversion of W phase: Speeding up seismic tsunami warning, *Geophys. J. Int.*, *175*(1), 222–238.

Lockridge, P. A., and R. H. Smith (1984), *Tsunamis in the Pacific Basin, 1900–1983*, Natl. Geophys. Data Cent., Boulder, Colo.

Madariaga, R. (1998), Sismicidad de Chile, Física de la Tierra 10: 221.

Melgar, D., B. W. Crowell, J. Geng, R. M. Allen, Y. Bock, S. Riquelme, E. M. Hill, M. Protti, and A. Ganas (2015), Earthquake magnitude calculation without saturation from the scaling of peak ground displacement, *Geophys. Res. Lett.*, *42*, 5197–5205, doi:10.1002/2015GL064278.

Melgar, D., et al. (2016), Local tsunami warnings: Perspectives from recent large events, *Geophys. Res. Lett.*, *43*, 1109–1117, doi:10.1002/2015GL067100.

Nealy, J. L., and G. P. Hayes (2015), Double point source W-phase inversion: Real-time implementation and automated model selection, Physics of the Earth and Planetary Interiors.

Ohta, Y., et al. (2012), Quasi real-time fault model estimation for near-field tsunami forecasting based on RTK-GPS analysis: Application to the 2011 Tohoku-Oki earthquake (M_w 9.0), *J. Geophys. Res.*, *117*, B02311, doi:10.1029/2011JB008750.

Rivera, L. A., H. Kanamori, and Z. Duputel (2011), W phase source inversion using the high-rate regional GPS data of the 2011 Tohoku-oki earthquake, In *AGU Fall Meeting Abstracts* (Vol. 1, p. 04).

Vidale, J. E., S. Goes, and P. G. Richards (1995), Near-field deformation seen on distant broadband seismograms, *Geophys, Res. Lett.*, *22*(1), 1–4, doi:10.1029/94GL02893.